Published in final edited form as:
Cancer Res. 2011 April 1; 71(7): 2428–2432. doi:10.1158/0008-5472.CAN-10-3484.

Novel human single chain antibody fragments that are rapidly interalizing effectively target epithelioid and sarcomatoid mesotheliomas

Arun K. Iyer[1], **Xiaoli Lan**[1], **Xiaodong Zhu**[2], **Yang Su**[1,2], **Jinjin Feng**[1], **Xiaoju Zhang**[2], **Dongwei Gao**[1], **Youngho Seo**[1], **Henry F. VanBrocklin**[1,3], **V. Courtney Broaddus**[3,4], **Bin Liu**[2,3,*], and **Jiang He**[1,3,*]

[1] Center for Molecular and Functional Imaging, Department of Radiology and Biomedical Imaging, University of California, San Francisco, CA 94143

[2] Department of Anesthesia, University of California, San Francisco, CA 94143

[3] Helen Diller Family Comprehensive Cancer Center, University of California, San Francisco, CA 94143

[4] Department of Medicine, University of California, San Francisco, CA 94143

Abstract

Human antibodies targeting all subtypes of mesothelioma could be useful to image and treat this deadly disease. Here we report tumor targeting of a novel internalizing human single chain antibody fragment (scFv) labeled with 99mTc (99mTc-M40) in murine models of mesothelioma of both epithelioid (M28) and sarcomatoid (VAMT-1) origins. 99mTc-M40 was taken up rapidly and specifically by both subtype tumor cells in vitro, with 68–92% internalized within 1h. The specificity of binding was evidenced by blocking (up to 95%) with 10-fold excess of unlabeled M40. In animal studies, tumors of both subtypes were clearly visualized by SPECT/CT as early as 1h post-injection of 99mTc-M40. Tumor uptake measured as percent of injected dose per gram tissue (%ID/g) at 3h was 4.38 and 5.84 for M28 and VAMT-1 tumors respectively, significantly greater than all organs or tissues studied (liver, 2.62%ID/g; other organs or tissues <1.7%ID/g), except the kidneys (130.7%ID/g), giving tumor-to-blood ratios of 5:1 and 7:1 and tumor-to-muscle ratios of 45:1 and 60:1, for M28 and VAMT-1 respectively. The target-mediated uptake was confirmed by a nearly 70% reduction in tumor activity following administration of 10-fold excess of unlabeled scFv. Taken together, these results indicate that M40 can rapidly and specifically target epithelioid and sarcomatoid tumor cells, demonstrating the potential of this agent as a versatile targeting ligand for imaging and therapy of all subtypes of mesothelioma.

Introduction

Malignant mesothelioma (MM), caused primarily by exposure to asbestos, is a highly aggressive tumor arising from serosal surfaces of the pleura, peritoneum and pericardium (1,2). MM has three major subtypes; epithelioid (EM) that is more likely to respond to treatment and accounts for 50–70% of all cases, sarcomatoid (SM) that rarely responds to any treatment and represents 7–20%, and mixed/biphasic for the remaining 20–30 %. MM has a median survival time of 8–14 months (3). There is an urgent unmet need to develop

*Correspondence should be addressed to: Jiang He, PhD, 185 Berry Street, Suite 350, San Francisco, CA 94143, Tel: 415-3533638, Fax: 415-5148242, Jiang.He@ucsf.edu, Or Bin Liu, PhD, 1001 Potrero Ave., 3C38, San Francisco, CA 94110, Tel: 415-2067963, Fax: 415 206 6276, liub@anesthesia.ucsf.edu.

new diagnostics and therapeutics for MM (4) as the disease has a long latency period with past and ongoing exposure to asbestos contributing to the development of new cases worldwide.

One approach to detect and treat cancer is to conjugate imaging and/or therapeutics to molecules which can recognize internalizing antigens, receptors or cell surface markers that are over-expressed on tumor cells, leading to efficient localization and tumor cell killing (5,6). However, presently there are very few MM-associated cell surface antigens that are over-expressed by all subtypes of MM, especially the SM (7). One well established marker —mesothelin, a 40kDa cell surface glycoprotein, has been reported to be expressed by EM cells (8), but not SM (9). Recently we have identified a panel of internalizing human scFv antibodies by phage display selection that target cell surface antigens associated with both EM and SM (6). The selected scFvs bind to human mesothelioma cells *in situ*, thereby recognizing clinically represented tumor antigens (6) and thus offer the potential to deliver high levels of imaging probes to tumor cells but not to non-target normal tissues based on intracellular delivery strategies. By screening the yeast surface human cDNA display library with mesothelioma targeting phage antibody, we have further identified MCAM/CD146/MUC18 as one of the target antigens for MM cells that was over-expressed in >80% of EM and SM tissues, but not other tissues (10). In the present study, we investigated both the *in vitro* and *in vivo* tumor targeting and imaging potential of an additional scFv (M40) for both EM (M28) and SM (VAMT-1) subtypes.

Materials and Methods

Expression and Purification of M40

The M40 was produced as previously reported (6,11–13).

^{99m}Tc Radiolabeling of M40

The scFv was radiolabeled as previously reported (14,16). The carbonyl-kit (IsoLink® Tyco/Mallinckrodt) was used to prepare the $[^{99m}Tc(CO)_3]$ moiety. An aliquot (40–60 μg) of M40 was mixed with 100–500 μL of $[^{99m}Tc(CO)_3(OH_2)_3]^+$ solution and the mixture was heated at 37°C for 60 min. The product was purified using a PD-10 column. Labeling efficiency and purity were determined by size-exclusion- HPLC and thin-layer-chromatography (TLC).

Fluorescence labeling of M40 (Cy5.5-M40)

The M40 was labeled with Cy5.5 by incubation with 3:1 molar excess of Cy5.5-NHS ester in a carbonate/bicarbonate buffer (pH 7.2–8.5) for 1 h followed by purification using PD-10 column.

In vitro cell culture assay

Internalization experiments were performed as described previously (12,15,16). Briefly, 1 million VAMT-1, M-28 or BPH-1 cells (control) were incubated with 0.05–2 μCi ^{99m}Tc-M40 in various concentrations for 1 h or 3 h. All cell lines had been tested for mycoplasma contamination and characterized by cell proliferation and morphology evaluation (6). The cells were washed to determine cell surface–bound (acid releasable) and internalized (acid resistant) radioligand/radioactivity expressed as the percentage of applied activity normalized to 1 million cells. For nonspecific uptake, the above procedure was repeated after addition of 10 fold excess unlabeled M40. For microscopy study, 1 μM (10 μl) of Cy5.5-M40 was incubated with tumor cells for 1 and 3 h. The cells were washed with PBS and then imaged using a TE2000-E Fluorescence Microscope (Nikon Inc., Japan) at 20× magnification.

Biodistribution studies

Animal procedures were performed according to a protocol approved by the UCSF Animal Care and Use Committee. Six-week-old male *nu/nu* mice were purchased from Charles River Laboratories. For tumor inoculation, 10^6 M-28 and VAMT-1 cells in 200 μL of PBS were administered subcutaneously into the right and left shoulders of the animal respectively. The mice were studied when tumor size reached ~3–5 mm in diameter (~20–60 mm^3 in volume). Tumor mice in groups of 4 animals were injected each with 18.5–37 MBq (0.5–1.0 mCi) of ^{99m}Tc-M40 containing ~2–4 μg of scFv. A control group (blocking study) were injected with 10 fold excess unlabeled M40 1h before ^{99m}Tc-M40. The biodistribution at 1, 3 or 6 h of the study group was determined and compared with that of the control group.

SPECT/CT imaging

Mice were imaged with a small animal SPECT/CT system (GE healthcare). For anatomical correlation, CT was first performed after injection. SPECT imaging was initiated 1h and 3h after injection.

PET/CT imaging

Mice were fasted overnight prior to ^{18}F-FDG injection of 3.7–7.4 MBq [100–200 μCi] and imaged with a microPET/CT system (Siemens Medical Solutions USA, Inc., PA) 1 h after injection for a 20 min acquisition time.

Results

In vitro characterization of ^{99m}Tc-M40

The ^{99m}Tc labeling yield of M40 (from $[^{99m}Tc(CO)_3(OH_2)_3]^+$) was 70–85%. The radiochemical purity of the ^{99m}Tc-M40 was greater than 95%. The final ^{99m}Tc-M40 had a high specific activity of ~9.3 MBq/μg (6.3×10^5 Ci/mol). The ^{99m}Tc radiolabeling was stable in phosphate buffer for at least the duration investigated (24 h), as reported previously (14,16).

The binding affinity of ^{99m}Tc-M40 to the mesothelioma cells exhibited an apparent Kd of 20–21 nM and the antigen density for M40 derived from the saturation cell binding assay was comparable on both tumor cells (Figure 1A, 1B). M40 was rapidly internalized over the concentrations tested with about 68–92% of total cell-associated following 1h incubation at 37°C (Figure 1C) whereas the binding and uptake in the control BHP cells was much less (Figure 1C). Specificity was further demonstrated by blocking of uptake/internalization into both M28 and VAMT-1 (>95%) cells with a 10-fold excess of unlabeled M40 (Figure 1C).

Fluorescence microscopy

As shown in Figure 1D, Cy5.5-M40 was rapidly internalized into mesothelioma cells within 1h after incubation at 37°C, whereas there was negligible uptake in the control (BPH-1) cells under identical conditions.

In vivo SPECT/CT imaging and biodistribution of ^{99m}Tc-M40

Mice were imaged with small animal SPECT/CT at 1h and 3h after injection with concomitant assessment of *ex vivo* biodistribution at 1h, 3h and 6h (Figure 2A). Imaging with SPECT/CT showed high tumor uptake (Figure 2B) as early as 3h post injection. At 3h, tumor uptake was 4.38 %ID/g and 5.84 %ID/g for M28 and VAMT-1 tumors respectively (Table 1), greater than for all organs/tissues studied (liver 2.62%ID/g, other organs/tissues <2 %ID/g) except the kidney (130.7%ID/g), giving M-28 and VAMT-1 tumor/muscle ratios

of 45:1, 60:1 and tumors/blood ratios of 5:1 and 7:1 respectively (Figure 2A). In contrast, the control blocking study with 10-fold excess of unlabeled M40 at 3h reduced by more than 70% of tumor uptake of the ^{99m}Tc-M40 to 0.9 %ID/g and 1.6%ID/g for M28 and VAMT-1 respectively (Table 1 and Figure 2C).

Micro-PET/CT imaging of ^{18}F-FDG

^{18}F-FDG PET imaging was performed to confirm the distinct identity of the two subtypes in single animal. As shown in Figure 2D, the ^{18}F-FDG PET/CT image at 1h detected SM (VAMT-1) preferentially.

Discussion

We report here the *in vitro* and *in vivo* tumor targeting and imaging potential of a rapidly internalizing human scFv (M40) selected from a panel of scFvs targeting internalizing epitopes present on both EM and SM cells (6).

Several important findings have been uncovered in this study. Firstly, the ^{99m}Tc-M40 showed strikingly rapid and selective binding and internalizing ability *in vitro* into the mesothelioma tumor cells but not into the control non-tumorigenic cells, consistent with our previous findings (6). Although we did not perform the Lindmo assay (17) to determine what percentage of our labeled antibodies retained reactivity (the immunoreactive fraction), our results nonetheless demonstrate that the M40 binds with high affinity to both subtypes of mesothelioma cells and that either the site-specific labeling of M40 with ^{99m}Tc through the hexahistidine tag or conjugation to Cy5.5 does not significantly affect its targeting ability. Secondly, while the M40 accumulated in the tumors, its clearance from blood and other normal organs was rapid (except from the kidney which is the site for all scFv clearance) making it feasible to label the M40 with positron-emitting residualizing radiometal isotopes with short half-lives such as gallium-68 (^{68}Ga) for quantitative PET imaging. Finally, unlike other available antibodies against MM, this antibody has the ability to target both EM and SM. If such dual targeting can be maintained in the clinical setting, this antibody would have a major imaging and therapeutic potential.

The ^{99m}Tc-M40 had a high uptake in the kidneys as observed with other ^{99m}Tc-scFvs (10,16), consistent with the route of scFv clearance *in vivo*. Nonetheless, additional engineering of M40 may further increase the kidney clearance rate and improve the contrast. In addition, developing other forms of the antibody such as diabody, minibody, or Affibody (Affibody AB) could further improve the tumor binding and homing efficiency as well as overall pharmacokinetic profile (10,18).

The ^{99m}Tc-M40 rapidly accumulated into both M28 and VAMT-1 cells as early as 3h with comparable tumor uptake at 4.38 ±0.39%ID/g) and 5.84±0.72ID%/g respectively. Because we observed the difference of ^{18}F-FDG uptake in our system between the two cell types, M28 and VAMT-1, with approximately 8%ID/g and 16%ID/g respectively similar to other reports (19,20), ^{18}F-FDG was used to confirm the identity of the two subtypes implanted in a single mouse and thus to highlight the dual targeting by M40. The characteristics of ^{99m}Tc-M40 are representative of a promising new class of radiotracers that recognize cell surface markers highly expressed at comparable level on both types of mesothelioma (Figure 1A & 1B). As such, they may find utility for tumor characterization and staging as well as treatment planning and monitoring complementary to ^{18}F-FDG.

In conclusion, we demonstrated that ^{99m}Tc-M40 selectively binds and internalizes into both M28 and VAMT-1 cells *in vitro*, and furthermore rapidly and specifically targets both

subtypes of mesothelioma *in vivo*, demonstrating its potential as a novel agent for imaging and therapy of all subtypes of mesothelioma.

Supplementary Material

Refer to Web version on PubMed Central for supplementary material.

Acknowledgments

The authors are grateful to Dr. Mary E. Dyszlewski at Tyco/Mallinckrodt for providing the carbonyl-kit (IsoLink®). This work is supported partially by NIH R01 CA135358 and the American Cancer Society (IRG-97-150-10) to Jiang He, and R01 CA118919 and R01 CA129491 to Bin Liu.

Abbreviations

MM	Malignant Mesothelioma
EM	Epithelioid Mesothelioma
SM	Sarcomatoid Mesothelioma

References

1. Robinson BW, Lake RA. Advances in malignant mesothelioma. N Engl J Med. 2005; 353:1591–603. [PubMed: 16221782]
2. Tsiouris A, Walesby R. Malignant pleural mesothelioma: current concepts in treatment. Nat Clin Pract Oncol. 2007; 4:344–52. [PubMed: 17534390]
3. Kindler H. Moving beyond chemotherapy: novel cytostatic agents for malignant mesothelioma. Lung Cancer. 2004; 45:125–7. [PubMed: 15196743]
4. Zheng G, Chen J, Li H, Glickson JD. Rerouting lipoprotein nanoparticles to selected alternate receptors for the targeted delivery of cancer diagnostic and therapeutic agents. Proc Natl Acad Sci U S A. 2005; 102:17757–62. [PubMed: 16306263]
5. Garnett MC. Targeted drug conjugates: principles and progress. Adv Drug Deliv Rev. 2001; 53:171–216. [PubMed: 11731026]
6. An F, Drummond DC, Wilson S, Kirpotin DB, Nishimura SL, Broaddus VC, et al. Targeted drug delivery to mesothelioma cells using functionally selected internalizing human single-chain antibodies. Mol Cancer Ther. 2008; 7:569. [PubMed: 18319332]
7. Zeng L, Fleury-Feith J, Monnet I, Boutin C, Bignon J, Jaurand MC. Immunocytochemical characterization of cell lines from human malignant mesothelioma: characterization of human mesothelioma cell lines by immunocytochemistry with a panel of monoclonal antibodies. Hum Pathol. 1994; 25:227–34. [PubMed: 7512071]
8. Hassan R, Bera T, Pastan I. Mesothelin: a new target for immunotherapy. Clin Cancer Res. 2004; 10:3937–42. [PubMed: 15217923]
9. Ordonez NG. The diagnostic utility of immunohistochemistry and electron microscopy in distinguishing between peritoneal mesotheliomas and serous carcinomas: a comparative study. Mod Pathol. 2006; 19:34–48. [PubMed: 16056246]
10. Bidlingmaier S, He J, Wang Y, An F, Feng J, Barbone D, et al. Identification of MCAM/CD146 as the Target Antigen of a Human Monoclonal Antibody that Recognizes Both Epithelioid and Sarcomatoid Types of Mesothelioma. Cancer Res. 2009; 69:1570. [PubMed: 19221091]
11. Liu B, Conrad F, Cooperberg M, Kirpotin D, Marks J. Mapping tumor epitope space by direct selection of single-chain Fv antibody libraries on prostate cancer cells. Cancer Res. 2004; 64:704. [PubMed: 14744788]
12. Roth A, Drummond DC, Conrad F, Hayes ME, Kirpotin DB, Benz CC, et al. Anti-CD166 single chain antibody-mediated intracellular delivery of liposomal drugs to prostate cancer cells. Mol Cancer Ther. 2007; 6:2737. [PubMed: 17938267]

13. Nielsen UB, Kirpotin DB, Pickering EM, Hong K, Park JW, Refaat Shalaby M, et al. Therapeutic efficacy of anti-ErbB2 immunoliposomes targeted by a phage antibody selected for cellular endocytosis. Biochim Biophys Acta. 2002; 1591:109–18. [PubMed: 12183061]

14. Waibel R, Alberto R, Willuda J, Finnern R, Schibli R, Stichelberger A, et al. Stable one-step technetium-99m labeling of His-tagged recombinant proteins with a novel Tc (I)-carbonyl complex. Nat Biotechnol. 1999; 17:897–901. [PubMed: 10471933]

15. Ruan W, Sassoon A, An F, Simko J, Liu B. Identification of clinically significant tumor antigens by selecting phage antibody library on tumor cells in situ using laser capture microdissection. Mol Cell Proteomics. 2006; 5:2364. [PubMed: 16982673]

16. He J, Wang Y, Feng J, Zhu X, Lan X, Iyer AK, et al. Targeting prostate cancer cells in vivo using a rapidly internalizing novel human single-chain antibody fragment. J Nucl Med. 2010; 51:427–32. [PubMed: 20150269]

17. Lindmo T, Boven E, Cuttitta F, Fedorko J, Bunn P Jr. Determination of the immunoreactive function of radiolabeled monoclonal antibodies by linear extrapolation to binding at infinite antigen excess. J Immunol Methods. 1984; 72:77–89. [PubMed: 6086763]

18. Olafsen T, Kenanova V, Wu A. Tunable pharmacokinetics: modifying the in vivo half-life of antibodies by directed mutagenesis of the Fc fragment. Nat Protoc. 2006; 1:2048–60. [PubMed: 17487194]

19. Tsuji AB, Sogawa C, Sugyo A, Sudo H, Toyohara J, Koizumi M, et al. Comparison of conventional and novel PET tracers for imaging mesothelioma in nude mice with subcutaneous and intrapleural xenografts. Nucl Med Biol. 2009; 36:379–88. [PubMed: 19423005]

20. Benard F, Sterman D, Smith RJ, Kaiser LR, Albelda SM, Alavi A. Metabolic imaging of malignant pleural mesothelioma with fluorodeoxyglucose positron emission tomography. Chest. 1998; 114:713–22. [PubMed: 9743156]

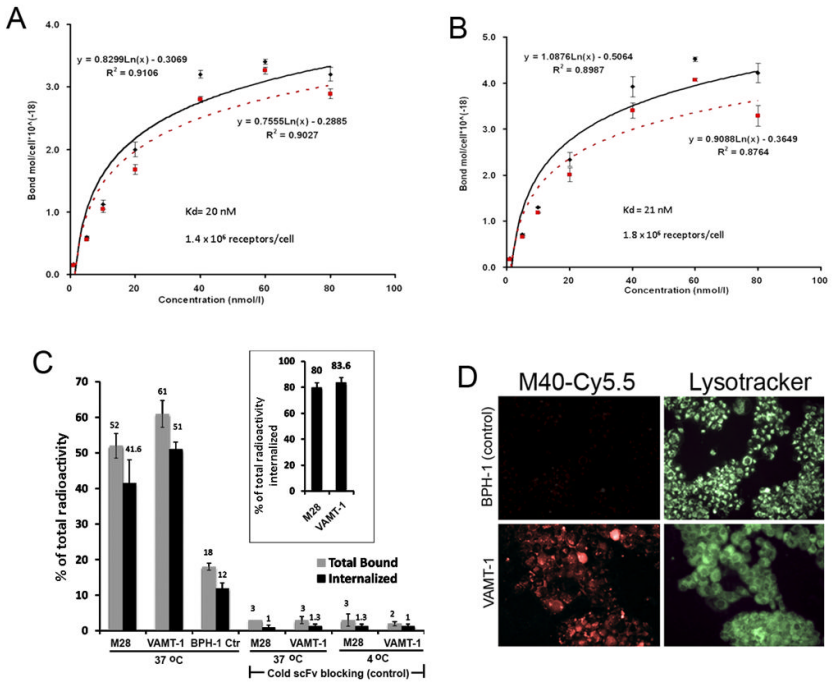

Figure 1.

In vitro cell binding and internalization of ^{99m}Tc-M40. **(A) & (B):** Binding (—) and internalization (--) curves of ^{99m}Tc-M40 at varying concentrations 1–80 nmol/L in M28 cells **(A)** and VAMT-1 cells **(B)** at 37°C at 1 h. **(C):** The ^{99m}Tc-M40 at a concentration of 20 nmol/L was incubated with 1×10^6 cells of M28, VAMT-1 or control (BPH-1) cells for 1 h at 37°C and 4°C. Blocking study was performed using 10 fold excess unlabeled M40 1 h prior to incubation with the ^{99m}Tc-M40 at 37°C. **Inset:** Internalization of total cell accumulation for ^{99m}Tc-M40 after 1 h incubation with M28 and VAMT-1 at 37°C. **(D):** Fluorescence microscopy of Cy5.5-M40 (red) on mesothelioma tumor cells (VAMT-1), and control cell line (BPH-1) at 1h incubation. The cells were stained with lysotracker (green) to demarcate the lyosomal compartments.

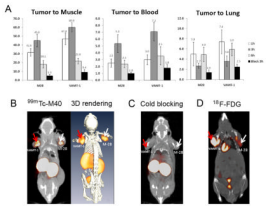

Figure 2.

In vivo tumor targeting of ^{99m}Tc-M40**. (A):** Tumor to non-target tissue ratios of ^{99m}Tc-M40. Tumor/Muscle **(Left)**, Tumor/Blood **(Middle)** and Tumor/Lung **(Right)** ratios in mice bearing both subtypes of mesothelioma tumors are shown at 1, 3, 6 h after injection and blocking study using the 10-fold excess unlabeled M40 1 h before ^{99m}Tc-M40 (Block 3 h). **(B):** SPECT/CT fused coronal image of ^{99m}Tc-M40 imaged 3 h after injection **(Left)**; 3D fused SPECT/CT coronal image **(Right); (C):** Blocking control study; **(D)**: PET-CT fused coronal image of ^{18}F-FDG imaged 1 h after injection.

TABLE 1

Biodistribution of ^{99m}Tc-M40. The biodistribution of ^{99m}Tc-M40 was assessed at 1, 3 and 6 h after injection in tumor bearing nude mice. A control (blocking) study was performed with 10-fold excess unlabeled M40 injected 1 h prior to injection of ^{99m}Tc-M40 in tumor bearing nude mice (n=4). Data are %ID/g ±SD.

Organ				Blocking
	1h	3h	6h	3h
Liver	2.43±0.08	2.62±0.34	2.48±0.22	2.40±0.21
Heart	0.26±0.10	0.28±0.03	0.23±0.01	0.21±0.07
Kidney	100.5±4.45	130.7±32.75	95.3±19.31	146.6±12.1
Lung	0.42±0.13	1.61±0.24	0.51±0.22	0.65±0.34**
Spleen	0.55±0.21	1.02±0.36	0.48±0.12	0.66±0.42
Pancreas	0.11±0.01	0.25±0.04	0.18±0.15	0.13±0.03**
Stomach	0.36±0.21	0.45±0.13	0.33±0.12	0.29±0.21
Sm. Int.	0.32±0.16	0.31±0.04	0.40±0.03	0.53±0.44
Lg. Int.	0.25±0.06	0.25±0.07	0.31±0.08	0.25±0.26
Muscle	0.06±0.02	0.10±0.05	0.10±0.03	0.17±0.11
Fat	0.11±0.01	0.13±0.03	0.06±0.01	0.11±0.10
Blood	1.20±0.21	0.82±0.13	0.81±0.15	2.40±0.21**
Tumor (VAMT-1)	3.74±0.07	5.84±0.72	2.60±0.19	1.62±0.16**
Tumor (M-28)	2.68±0.24	4.38±0.39	2.17±0.21	0.91±0.22**

** indicates organs with significant difference in uptake at 3 h after injection between study group and blocking control group ($P<0.05$).